

# Parameterization of Mesoscale Stationary Orographic Wave Forcing for Use in Numerical Models of Atmospheric Dynamics

N. M. Gavrilov and A. V. Koval

*St. Petersburg State University, ul. Ul'yanovskaya 1, Petrodvorets, St. Petersburg, 198504 Russia*

*e-mail: gavrilov@pobox.spbu.ru, koval\_spbu@mail.ru*

Received December 13, 2011; in final form, May 29, 2012

**Abstract**—Polarization relations for mesoscale stationary orographic waves (MSOWs) and formulas for calculating vertical profiles of the total vertical flux of wave energy and amplitudes of horizontal speed are obtained by taking account the rotation of the atmosphere. Expressions are derived for the total wave heat flux, accelerations of the mean flow, and heat influxes generated by MSOWs. Calculations of the characteristics of MSOWs propagating in the atmosphere from the surface to the lower thermosphere are made. It was shown that MSOWs may significantly affect the circulation and thermal regime of the middle and upper atmosphere.

**Keywords:** atmospheric dynamics, mesoscale waves, orography, wave acceleration, heat influx, parameterization

**DOI:** 10.1134/S0001433813030067

## 1. INTRODUCTION

Internal gravity waves (IGWs) play an important role in the formation of the general circulation, thermal regime, and composition of the middle and upper atmosphere. Interest in studying accelerations of the mean flow and heat influxes generated by IGWs has increased in recent years due to numerical modeling of the general circulation of the atmosphere. Interpreting IGW observations and including IGW effects in numerical atmospheric models necessitate the development of simple numerical schemes that would satisfactorily describe the wave oscillations and demand minimal computer time.

The topography of the earth's surface is one important source for IGWs. The incoming airflow interacts with irregularities of the relief so that mesoscale stationary orographic waves (MSOWs) can arise. Quasi-stationary orographic waves have been observed in the troposphere [1, 2] and the stratosphere [3–5] via various techniques. Stationary wave structures with horizontal lengths of about 36 km aligned parallel to the Andes mountain system and having the properties of orographically generated gravity waves propagating up into the upper atmosphere were visible in the images of nighttime airglow emissions at 80- to 100-km altitudes over Argentina [6].

Orographic waves and their potential impact on the thermal regime and dynamics of the mesosphere and lower thermosphere have been studied extensively by Russian scientists over the Ural Mountains [7–9] and the Caucasus range [10, 11]. These experimental data demonstrate the existence of quasi-stationary temper-

ature disturbances with amplitudes of  $\sim 10$  K over mountain systems at 80–90 km. Estimates of the spatial distribution of energy fluxes of orographic waves into the mesopause region in the lee of a mountain range were made in [12]. The wave-energy fluxes were estimated in [12] to be  $\sim 3$  mW/m<sup>2</sup> on average. The possibility that orographic waves could influence the circulation and thermal regime of the middle atmosphere was discussed in [13–16]. The mesoscale variability of temperatures in the troposphere and stratosphere was analyzed and its enhancement over mountain systems was demonstrated in [17] using low-orbit GPS satellite data.

Several parameterizations have been developed for MSOWs, for example, [18, 19], but these parameterizations do not take into account all the details of the propagation and impact of the waves in the atmosphere. In [18] most attention has been given to the parametrization of the earth's surface relief and to the estimation of parameters of MSOWs near their sources, but parameters of the waves at high altitudes have not been considered. In [19], the dissipation of MSOWs in the atmosphere is disregarded. This simplification is permissible in calculations of the vertical profiles of tropospheric MSOWs, but the dissipation of wave energy becomes significant as the altitude increases. Furthermore, several parameterizations do not calculate vertical profiles of heat fluxes and wave accelerations induced by MSOWs, correct formulas for which can be obtained only by taking into account the rotation of the atmosphere.

In this study we have developed a parametrization for MSOWs propagating in the atmosphere from the earth's surface, improved polarization relations for MSOWs, and derived formulas to calculate the total vertical flux of wave energy and the amplitude of horizontal speed that take into account the rotation of the atmosphere.

## 2. DYNAMIC AND THERMAL EFFECT OF OROGRAPHIC WAVES

According to the theory of mesoscale stationary disturbances arising when an incoming airstream flows over a mountain, these disturbances can be referred to as IGWs with frequencies  $\sigma = 0$ . When the IGWs propagate in an inhomogeneous rotating atmosphere with dissipation, the mean flow and the waves exchange energy and the atmosphere is warmed by the dissipation of IGW energy. From [20], the wave-energy balance equation for stationary and horizontally homogeneous wave-period-averaged quantities can be written as

$$\begin{aligned} \frac{\partial F_E}{\partial z} &= -\bar{\rho}D - \overline{\rho v_\alpha a_{w\alpha}}, \\ a_{w\alpha} &= -\frac{1}{\bar{\rho}} \frac{\partial(\bar{\rho} v'_\alpha w')}{\partial z}, \\ F_E &= \overline{p'w'} + \overline{\rho v_\alpha v'_\alpha w'} - (\sigma'_{z\beta} + \tau'_{z\beta})v'_\beta, \end{aligned} \quad (1)$$

where  $p$  and  $\rho$  are the atmospheric pressure and density, respectively;  $v_\alpha$  and  $w$  are the velocity components along the horizontal axes  $x_\alpha$  and the vertical axis  $z$ , respectively; repeated Greek subscripts assume summation;  $F_E$  is the total wave-energy flux, which includes the flux of wave energy and its transport by the mean flow and by turbulent and molecular diffusion;  $D$  is the dissipation rate of wave energy;  $a_{w\alpha}$  is the components of the wave acceleration of the mean flow that enter the equation for the horizontal component of the mean velocity;  $\sigma_{\alpha\beta}$  and  $\tau_{\alpha\beta}$  are the molecular and turbulent viscous stress tensors, respectively; the overbar denotes averaging over a wave period; and primes denote wave components of the corresponding quantities.

On the right-hand side of the first equation in (1), there are terms that describe the dissipation rate of wave energy and the work of nonlinear wave–mean flow interaction forces, which depends on the velocity of the mean flow and wave acceleration. For a correct description of the energetics of the dynamic processes considered here, it is important to know the relation between the indicated sources and sinks of wave energy. It is shown in [20] that analytical expressions relating the rate of wave-energy dissipation and wave accelerations can be obtained if there is a vertical gradient of the mean wind. These expressions serve as a basis for our research.

When we consider the propagation of plane monochromatic wave components, it is convenient to direct one horizontal axis  $\xi$  along the horizontal wave vector  $\mathbf{k}$  and the other axis  $\eta$  normally to  $\mathbf{k}$ . For the component of the wave acceleration generated by a plane IGW along the  $\xi$  axis, the following formula may be obtained in a stationary horizontally uniform model for the height-varying mean wind ( $\partial \bar{v}_\xi / \partial z \neq 0$ ) in [20]:

$$\begin{aligned} a_{w\xi} &= \frac{k}{\sigma - k \bar{v}_\xi} \left\{ D - \frac{1}{\bar{\rho}} \frac{\partial}{\partial z} \left[ \overline{(\sigma_{z\beta} + \tau_{z\beta}) v'_\beta} - \left( \frac{\partial \bar{v}_\xi}{\partial z} \right)^{-1} \right. \right. \\ &\quad \left. \left. \times \left( \frac{p'}{\bar{\rho}} + v'_\xi \left( \bar{v}_\xi - \frac{\sigma}{k} \right) \right) \frac{\partial(\sigma_{\alpha\xi} + \tau_{\alpha\xi})}{\partial x_\alpha} \right] \right\}, \end{aligned} \quad (2)$$

and the total heating rate due to IGW energy dissipation and transport is described by

$$\varepsilon_w = D + \bar{v}_\xi a_{w\xi} - \frac{1}{\bar{\rho}} \frac{\partial}{\partial z} \left[ \frac{(\gamma - 1) \bar{\rho} T}{gB} (\varepsilon'_t + \varepsilon'_m + \varepsilon'_r) s' \right], \quad (3)$$

where  $B = (\gamma - 1) + g^{-1} \partial c^2 / \partial z$  is the parameter of statistical stability of the atmosphere;  $\gamma = c_p / c_v$  is the ratio of heat capacities;  $T$  is the temperature;  $g$  is the acceleration due to gravity;  $\varepsilon'_t$ ,  $\varepsilon'_m$ ,  $\varepsilon'_r$  are the wave components of heat influxes due to turbulent and molecular viscosity and radiative heat exchange, respectively;  $s'$  is the wave component of entropy; and  $c$  is the speed of sound. Using a standard theory of atmospheric waves in a plane rotating atmosphere (e.g., [21]), it is possible to derive polarization relations for stationary gravity waves with frequencies  $\sigma = 0$  and rather high vertical and horizontal wave numbers  $|m| \gg 1/(2H)$  and  $k^2 \gg f^2/c_s^2$  (where  $H$  is the height of a uniform atmosphere,  $c_s$  is the speed of sound, and  $f$  is the Coriolis parameter). These polarization relations can be written as

$$\begin{aligned} U &= -k^2 \bar{v}_\xi^2 c_s^2 m X; \quad V = i f k c_s^2 m X; \quad W = \bar{v}_\xi k^3 c_s^2 X; \\ R &= [(k^2 \bar{v}_\xi^2 - f^2) m + i k^2 c_s^2 N^2 / g] X; \\ P &= \gamma c_s (k^2 \bar{v}_\xi^2 - f^2) m X; \\ \Theta &= [(\gamma - 1)(k^2 \bar{v}_\xi^2 - f^2) m - i k^2 c_s^2 N^2 / g] X, \end{aligned} \quad (4)$$

where  $U$ ,  $V$ , and  $W$  are the amplitudes of fluctuations of the velocity components along the axes  $\xi$ ,  $\eta$ , and  $z$ ;  $R$ ,  $P$ , and  $\Theta$  are the amplitudes of relative density, pressure, and temperature variations, respectively; and  $X$  is an arbitrary constant. A comparison of the first two formulas of (4) show that, for the wave components with  $|k| \gg f / |\bar{v}_\xi|$ , the amplitude of fluctuations of the velocity  $U$  along the  $\xi$  axis parallel to the wave vector  $\mathbf{k}$  far exceeds the amplitude of the velocity  $V$  in the perpendicular direction and this “transverse”

velocity component can be ignored. Using (4) and the relations for  $\sigma_{\alpha\beta}$ ,  $\varepsilon_t + \varepsilon_m$ , and  $\varepsilon_r$  from [20] in (1) and (3), one can obtain the following expressions for the total wave-energy flux, wave acceleration along the  $\xi$  axis, and the total heating rate caused by stationary waves:

$$F_E = \left( -\frac{\bar{\rho} f^2 U^2}{2mk\bar{v}_\xi} \right); \quad m^2 = \frac{N^2}{\bar{v}_\xi^2} \left( 1 - \frac{f^2}{k^2 \bar{v}_\xi^2} \right)^{-1}$$

$$a_{w\xi} = -\frac{m^2 U^2}{2\bar{v}_\xi} (\nu + K_z) \left( 1 + \frac{1}{(\gamma - 1)Pr} \right), \quad (5)$$

$$\varepsilon_w = (\nu + K_z) \delta m^2 U^2, \quad \delta = \frac{f^2}{k^2} \frac{\partial}{\partial z} \left( \frac{\partial \bar{v}_\xi^2}{\partial z} \right)^{-1},$$

where  $\nu$  and  $K_z$  are the kinematic coefficients of molecular and turbulent viscosity, respectively, and  $Pr$  is the effective Prandtl number equal to the ratio of the total coefficients of molecular and turbulent viscosity and heat conduction. When deriving the expression for  $\varepsilon_w$  in (5), we remember that  $D$  is canceled after the substitution of (2) into (3) for stationary waves and pick up the main summand of the remaining divergent components. From the last two relations of (5), it is seen that, in the suggested parametrization for stationary mesoscale waves,  $\varepsilon_w/a_{w\xi} = (1 - \gamma)\delta\bar{v}_\xi/\gamma$ . When  $\delta = 1$ , the expression for  $\varepsilon_w$  in (5) coincides with that for the rate of dissipation of wave energy due to molecular and turbulent viscosity, which is often used to estimate the thermal effect of stationary mesoscale waves. From (1) and the first relation of (5), one can obtain an equation describing the variation in  $U^2$  with height, which, with an accuracy to the largest term on the right-hand side, has the form

$$\frac{\partial}{\partial z} \left( \frac{\bar{\rho} f^2 U^2}{2|k|N} \sqrt{1 - \frac{f^2}{k^2 \bar{v}_\xi^2}} \right) = -\bar{\rho}(\nu + K_z) \delta m^2 U^2. \quad (6)$$

A comparison of this equation with the last formula of (5) shows that the divergence of the upward total MSOW energy flux is proportional to  $-\varepsilon_w$ . It is usually assumed that  $\delta > 0$  and the dissipation of wave energy leads to atmospheric warming,  $\varepsilon_w > 0$ , and to a decrease in the total flux of wave energy with height. According to (5), for specific vertical profiles of the mean wind, areas are possible in which  $\delta < 0$  and the total wave-energy flux must increase with height in accordance with (6). Such an enhancement of the energy outflow may lead in (5) to  $\varepsilon_w < 0$  and to a local cooling of the atmosphere.

When the amplitude of the wave at the lower boundary is specified, Eq. (6) can be solved with respect to  $U^2$  for the given vertical profiles  $\bar{v}_\xi$  and  $\bar{T}$ . Then from (5) we can calculate the wave acceleration  $a_{\xi w}$  and the total heating rate  $\varepsilon_w$ , which can be used to

take into account the dynamic and thermal effects of stationary gravity waves in atmospheric dynamic models.

### 3. NUMERICAL ALGORITHM AND PARAMETRIZATION OF OROGRAPHY

Most numerical general circulation models of the middle atmosphere use a finite-difference grid along the vertical coordinate with a spacing  $\Delta z$ . Solving (6) within the  $i$ th spacing, one can obtain the expression relating  $U_{i+1}^2$  at the  $(i+1)$ th grid point to  $U_i^2$ , which has the following form:

$$U_{i+1}^2 = \frac{r_i}{r_{i+1}} U_i^2 \exp \left[ \left( \frac{s_i}{r_i} \right) \Delta z \right] \quad (7)$$

$$r_i = \frac{\bar{\rho} f^2}{2|k|N_i} \sqrt{1 - \frac{f^2}{k^2 \bar{v}_\xi^2}}, \quad s_i = \bar{\rho}_i (\nu_i + K_{zi}) m_i^2 \delta_i,$$

where the subscript  $i$  denotes the values of quantities at the level  $z = z_i$ .

A constant surface atmospheric current flowing over mountains or other solid barriers may be an important source of stationary mesoscale waves in the atmosphere. For a parametrization of mesoscale orography, in our study we use a modification of the method developed in [19]. This method uses the concept of subgrid orography, which considers variations in the elevation of the earth's surface with horizontal scales smaller than the horizontal grid spacing of a numerical model.

In the parametrization we develop here, the elevation scale  $h'$ , which describes subgrid topography, is determined from the formula  $h' = L_l(h) - L_h(h)$ . Here  $L_l(h)$  and  $L_h(h)$  are the low-frequency and high-frequency numerical filters applied to the actual distribution of the earth's surface elevations  $h$ . These filters use averaging over areas of the earth's surface with Gaussian weight functions. Characteristics of the filters are chosen to pass variations in the earth's surface elevation having horizontal scales 20–200 km, which is recommended for parameterizations of orographic IGWs in [19]. In the neighborhood of each grid point, the elliptical approximation of subgrid-scale orography is used following [18]

$$h(x', y') = \frac{h_m}{1 + (x'/a)^2 + (y'/b)^2}, \quad (8)$$

where  $h_m$  is the effective elevation of an inhomogeneity,  $a$  and  $b$  are the major and minor semi-axes of an ellipse, and  $x'$  and  $y'$  are the coordinate axes directed along these semi-axes, respectively (Fig. 1). The forces acting on an elliptical mountain barrier from the incoming horizontal flow were studied in [22]. The mountain barrier acts on the atmosphere with equal and oppositely directed forces. These forces are equivalent to the vertical horizontal momentum flux  $F_m$

generated by MSOWs. The components of this flux (per unit area) directed toward the incoming flow ( $F_m$ ) and normally to it ( $F_{mn}$ ) are given by

$$\begin{aligned} F_{mv} &= \rho_0 v_0 N_0 \mu s G (B \cos^2 \chi + C \sin^2 \chi), \\ F_{mn} &= \rho_0 v_0 N_0 \mu s G (B - C) \sin \chi \cos \chi, \end{aligned} \quad (9)$$

where the subscript 0 denotes values of the quantities in the surface layer of the atmosphere,  $v_0$  is the modulus of the mean velocity of horizontal wind at the lower boundary,  $\mu = \langle h^2 \rangle - \langle h \rangle^2$  is the variance of variations in the earth's surface elevation,  $\chi$  is the angle between the direction of the wind and the minor axis of the elliptical relief (Fig. 1),  $s^2 = \langle (\partial h / \partial x')^2 \rangle$  is the slope parameter, and  $G$  is the so-called parameter of the mountain sharpness. According to [18],  $G = 1.21$  for the mountain profile (8). The coefficients  $B$  and  $C$  in (9) are calculated from the formulas  $B = 1 - 0.18\eta - 0.04\eta^2$ ,  $C = 0.48\eta + 0.3\eta^2$ , where  $\eta^2 = \langle (\partial h / \partial y')^2 \rangle / \langle (\partial h / \partial x')^2 \rangle$  is the parameter characterizing the anisotropy of subgrid-scale orography. Here the angular brackets denote averaging over a selected horizontal area centered at a given point of a medium and over altitude intervals equal to the effective elevation of the elliptical relief  $h_m$  in (8). The theory of orographic waves [21] gives the following expression for the modulus of the vertical flux of horizontal momentum in a plane rotating atmosphere:

$$F_m = \rho_0 v_0 N_0 k_e \mu^2 \cos \chi / 2, \quad (10)$$

where  $k_e$  is the effective horizontal wave number. Taking into account (9) for the components of the wave momentum flux in (10), we obtain the following expression for the effective horizontal wave number of an orographic wave:

$$k = k_e = \frac{s \sqrt{F_{mv}^2 + F_{mn}^2}}{2 \rho_0 v_0 N_0 \mu^2 \cos \chi}. \quad (11)$$

Using polarization relations (4), we can obtain

$$F_m = \rho_0 \overline{v'_\xi w'} = \rho_0 U_0^2 \sqrt{\frac{k^2 \overline{v_{\xi 0}^2} - f^2}{2 N_0}}. \quad (12)$$

By calculating  $F_m$  on the left-hand side of (12) from (9), it is possible to determine the effective amplitude  $U_0$  of the orographic wave at the lower boundary, which is required to solve Eq. (6) using the algorithm (7). The values of  $k$  and  $U_0$  calculated from (11) and (12) may be used as a boundary condition for calculating the effective orographic-wave amplitude  $U$  from (7) at all points of the vertical grid. The mean-wind component in the direction of the wave  $\overline{v'_\xi}$  in (5) and (6) is found as the sum of projections of the mean zonal and meridional wind onto the direction of the wave momentum flux calculated from (9). After having calculated the  $U$  profile, we use (5) to calculate

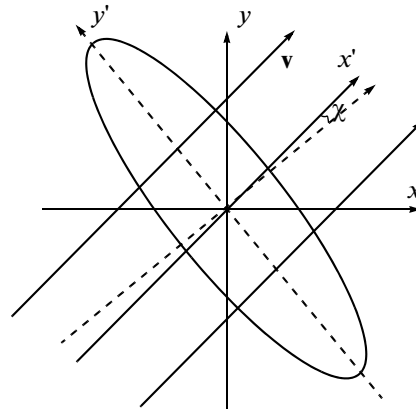


Fig. 1. Scheme of the orientation of the effective elliptical relief on the horizontal plane. The coordinate axes  $x$  and  $y$  are directed eastward and northward; the  $x'$  and  $y'$  axes are directed along the minor and major axes of the elliptical mountain profile, respectively; and the vectors  $v$  denote the direction of the incoming mean flow.

vertical profiles of the wave acceleration and the wave influx of heat.

#### 4. VERIFICATION CALCULATIONS

In performing illustrative calculations to verify the efficiency of the parametrization described above, we used the 2-min gridded Earth Topography data set (ETOPO2). The horizontal grid fits the COMMA-SPBU (Cologne Model of the Middle Atmosphere at St. Petersburg University) model of general circulation of the middle atmosphere [23] and has 36 grid points along the meridians and 64 grid points along the parallels. The vertical grid spacing is 4.5 km. Calculations were made at altitudes from the ground to 100 km. Vertical mean profiles of temperature and zonal and meridional winds in the atmosphere were calculated from the MSISE90 [24] and HWM93 models. The mean zonal and meridional winds in the surface layer of the atmosphere were taken from the National Center for Atmospheric Research (NCAR) reanalysis data based on observations of the global meteorological network [25]. In the expression for  $\epsilon_w$  in (5), constant value  $\delta = 1$  was given for simplicity, which corresponds to the widely used expression for the rate of wave-energy dissipation due to molecular and turbulent viscosity. The exponentially growing total coefficients of turbulent and molecular kinematic viscosity and  $Pr = 1$  were specified. Calculations were made for January.

Figures 2 and 3 show the vertical profiles of the amplitude of orographic waves, the total heating rate of the waves, the modulus of the wave acceleration, relative variations in temperature, vertical wave number, energy flux, and mean temperature and projection of wind velocity onto the direction of the wave vector at different geographic locations. Figure 2 corresponds

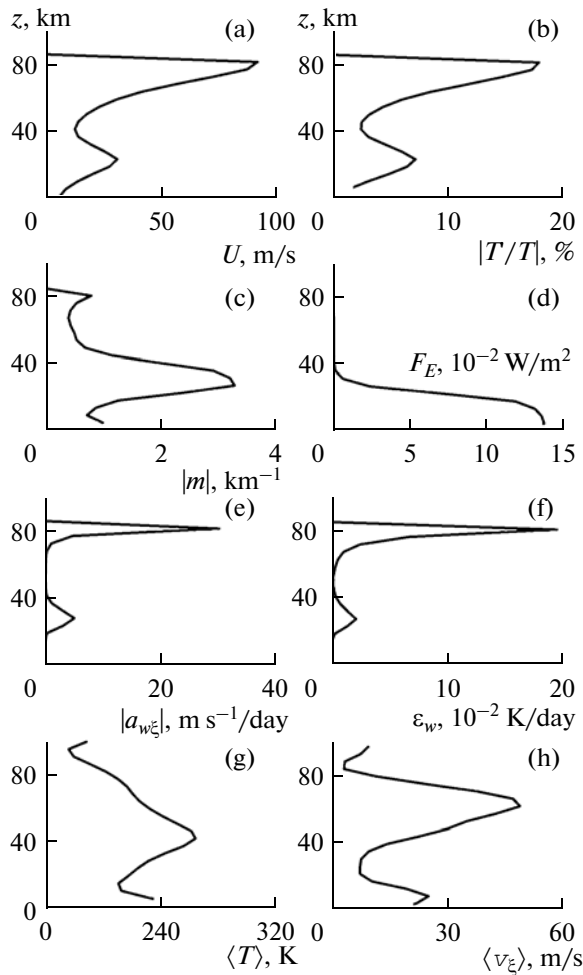


**Fig. 2.** Calculated vertical profiles of the parameters of an orographic wave: (a) velocity amplitude, (b) amplitude of relative variations in temperature, (c) modulus of the vertical wave number, (d) total vertical flux of wave energy, (e) modulus of the wave acceleration, (f) wave heat flux, and mean profiles of (g) temperature and (h) zonal wind used in the calculations at  $32.5^\circ$  N,  $101^\circ$  E in January.

to the Alpine region of the Himalayas with an average elevation  $\langle h \rangle \approx 3.8$  km and the variance of the earth's surface elevations  $\mu \approx 0.9$  km. The terrain corresponding to Fig. 3 has a lower average elevation  $\langle h \rangle \approx 2$  km and  $\mu \approx 1.6$  km. (1) The larger value of  $\mu$  and the higher air density at lower altitudes of orographic wave generation result in larger values of wave energy flux  $F_E$  at low altitudes in Fig. 3d than in Fig. 2d. At high altitudes in Fig. 2a, the MSOW amplitude increases up to 75–80 km, while in Fig. 3a it decreases sharply above 25–30 km. Such a difference in the behavior of the waves can be explained by the larger vertical wavelength in the first case than in the second. This can be seen from a comparison of Figs. 2c and 3c, which depict profiles of the vertical wavenumber. It follows from (5)–(7) that the increase in  $|m|$  leads to a stronger dissipation

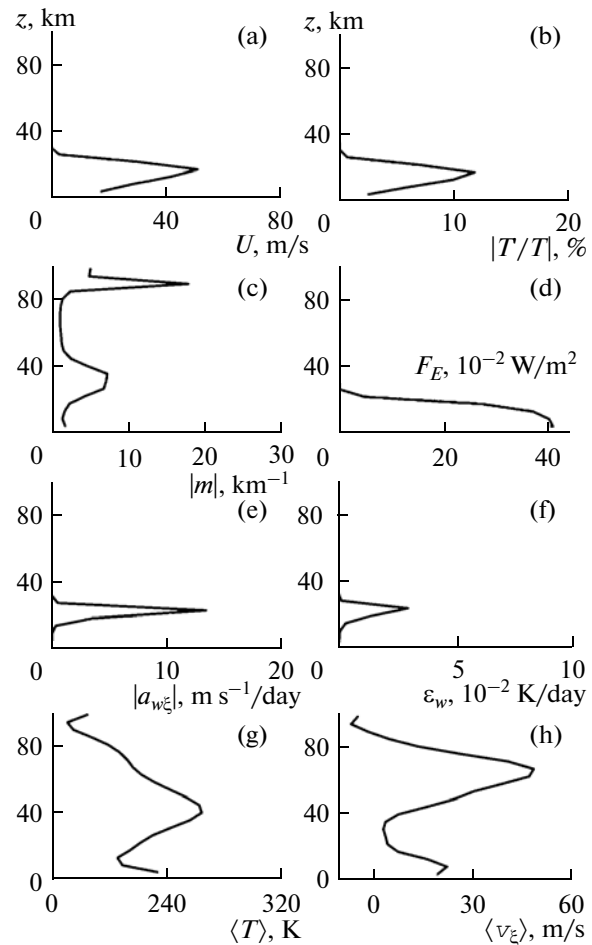


**Fig. 3.** The same as in Fig. 2, but for the latitude  $27.5^\circ$  N and longitude  $95.6^\circ$  E.

and to the decay of short orographic waves with altitude.

The distribution of the earth's surface elevation variance  $\mu$  is shown in Fig. 4. The largest variance is observed over mountain systems. This follows from the formula for the variance considered in Section 3. Figures 5 and 6 are the latitude–longitude distributions of the logarithm of the amplitude of MSOW velocity in the surface layer of the atmosphere and at 72 km, respectively. In Fig. 4, the regions of maximum amplitudes correspond to the geographic distribution of the mountain systems.

The vertical profiles of the orographic wave amplitudes depend very much on the profiles of the mean wind, temperature, turbulent and molecular viscosity, and heat conduction. With little dissipation near the ground, orographic wave amplitudes increase quasi-exponentially with altitude, the regions of maximum MSOW amplitudes in Fig. 4 being well correlated with the mountain systems.

At high altitudes, the kinematic viscosity and heat conduction increase and cause the dissipation of

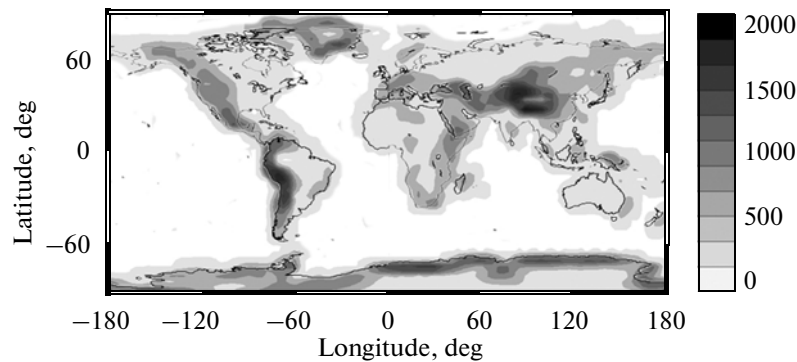


Fig. 4. Latitude–longitude distribution of the variance of variations in the earth's surface elevation (in m).

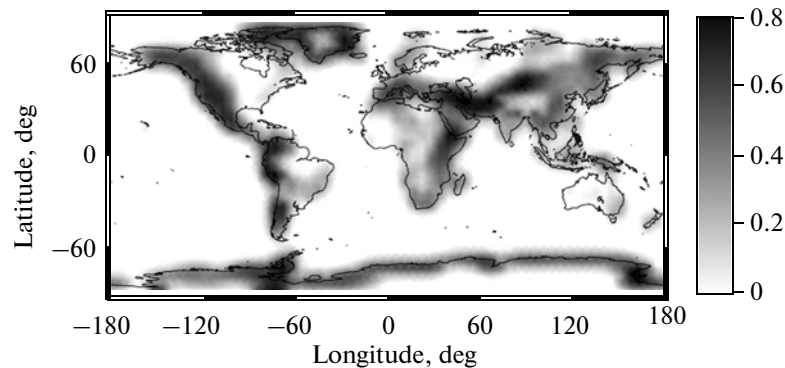


Fig. 5. Latitude–longitude distribution of the logarithm of the amplitude of MSOW velocity variations in the surface layer in January (in m/s).

MSOWs with small vertical wavelengths. In Fig. 6 for altitude 72 km, therefore the regions of increased MSOW amplitudes are not always located over major mountain systems and also reflect the structure of the background wind and temperature profiles, which influence the MSOW propagation in the atmosphere. In Fig. 6, in particular, there are more regions with increased MSOW amplitudes at the middle and high latitudes of the Northern (winter) Hemisphere than at the analogous latitudes of the Southern (summer) Hemisphere. This may be caused by the more favorable conditions of MSOW propagation in the winter structures of background temperature and wind than in the summer ones [15]. In particular, a change in the direction of zonal circulation in the summer stratosphere and mesosphere can produce critical levels of strong MSOW absorption at altitudes where  $\bar{u} = f/k$ , which can prevent the waves from penetrating into the upper atmosphere. The calculations show that the vertical wave-energy fluxes, wave accelerations of the mean flow, and heat influxes have spatial distributions analogous to those of the MSOW amplitudes in Figs. 5 and 6 for the corresponding altitudes.

The temperature perturbation amplitudes of orographic waves at 80–90 km over mountain systems in Fig. 2b are 10–30 K, and the total vertical wave-

energy flux  $F_E$  is a few milliwatts per square meter, which in the order of magnitude comparable with the experimental estimates [10–12] (see Introduction). The wave accelerations of the mean flow in the mesosphere and lower thermosphere in Fig. 2e may be as large as several tens of  $\text{m s}^{-1}/\text{day}$ , and the wave heat influxes in Fig. 2f may reach several K/day. This confirms the conclusions of [13–16] that orographic waves may significantly affect the circulation and thermal regime of the middle atmosphere.

As was shown above, the calculations in this paper used constant values of  $\text{Pr}$  and  $\delta$  in (5)–(7). In fact, according to the last formula of (5), the use of constant  $\delta$  corresponds to the assumption that  $k$  depends on the profile of the mean wind. For more accurate estimates of the dynamic and thermal effects of stationary mesoscale waves, the dependence of  $\text{Pr}$ ,  $\delta$ ,  $\nu$ , and  $K_z$  on the mean wind and temperature distributions and, perhaps, on the MSOW parameters must be taken into account.

## 5. CONCLUSIONS

In this study polarization relations for MSOWs were improved and formulas for calculating the total vertical flux of wave energy and the vertical profile of

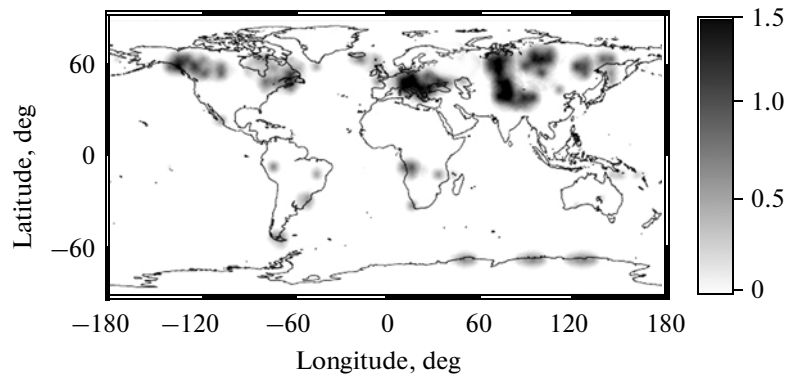


Fig. 6. The same as in Fig. 5, but at an altitude of 72 km.

the amplitude of horizontal velocity were derived using the theory of mesoscale waves in a rotating atmosphere. Expressions were obtained for the total wave heat flux, accelerations of the mean flow, and heat influxes induced by stationary wave harmonics of orographic origin. The parametrization of stationary orographic waves generated by surface airstreams flowing over a mountain relief was modified. Calculations of the characteristics of orographic waves propagating in the atmosphere from the ground to the lower thermosphere were calculated. Results of previous studies demonstrating that orographic waves may significantly influence the circulation and thermal regime of the middle and upper atmosphere were confirmed. The formulas derived in this study may be useful for the parametrization of the dynamic and thermal effect of stationary orographic waves in atmospheric dynamic models.

#### ACKNOWLEDGMENTS

We thank our reviewers for helpful comments that have significantly improved the text of the paper. This study was supported in part by the Russian Foundation for Basic Research.

#### REFERENCES

1. R. S. Scorer, "Theory of waves in the lee of mountains," *Quart. J. R. Meteorol. Soc.* **75** (323), 41–56 (1949).
2. T. Beer, *Atmospheric Waves* (Wiley, New York, 1974).
3. S. D. Eckermann and P. Preusse, "Global measurements of stratospheric mountain waves from space," *Science* **286**, 1534–1537 (1999).
4. P. Preusse, A. Dornbrack, S. D. Eckermann, M. Riese, B. Schaeler, J. T. Bacmeister, D. Broutman, and K. U. Grossman, "Space-based measurements of stratospheric mountain waves by CRISTA: 1. Sensitivity, analysis method, and a case study," *J. Geophys. Res.* **107** (D23), 8178 (2002). doi 10.1029/2001JD000699
5. J. H. Jiang, D. L. Wu, and S. D. Eckermann, "Upper atmosphere research satellite (UARS) observation of mountain waves over the Andes," *J. Geophys. Res.* **107** (D20), 8273 (2002). doi 10.1029/2002JD002091
6. S. Smith, J. Baumgardner, and M. Mendillo, "Evidence of mesospheric gravity-waves generated by orographic forcing in the troposphere," *Geophys. Res. Lett.* **36**, L08807 (2009). doi 10.1029/2008GL036936
7. A. I. Semenov, M. V. Shagaev, and N. N. Shefov, "On the influence of orographic waves on the upper atmosphere," *Izv. Akad. Nauk SSSR, Fiz. Atmos. Okeana* **17** (9), 982–984 (1981).
8. N. N. Shefov, N. N. Pertsev, M. V. Shagaev, and V. N. Yarov, "Orography-induced variations in the upper atmosphere emission," *Izv. Akad. Nauk SSSR, Fiz. Atmos. Okeana* **19** (9), 920–926 (1983).
9. N. N. Shefov and N. N. Pertsev, "Orographic disturbances of upper atmosphere emissions," in *Handbook for Middle Atmosphere Program (MAP). Scientific Committee on Solar–Terrestrial Physics (SCOSTEP)* (University of Illinois, Urbana, 1984), Vol. 10, pp. 171–175.
10. V. A. Sukhodoev, V. I. Perminov, L. M. Reshetov, et al., "Orographic effect in the upper atmosphere," *Izv. Akad. Nauk SSSR, Fiz. Atmos. Okeana* **25** (9), 926–932 (1989).
11. V. A. Sukhodoev and V. N. Yarov, "Temperature variations of the mesopause in the leeward region of the Caucasus Ridge," *Geomagn. Aeron.* **38** (4), 545–548 (1998).
12. N. N. Shefov, A. I. Semenov, N. N. Pertsev, et al., "Spatial distribution of IGW energy inflow into the mesopause over the lee of a mountain ridge," *Geomagn. Aeron.* **39** (5), 620–627 (1999).
13. A. A. Blank, "Estimate for the temperature of heating induced by dissipation of leeward mountain waves," *Izv. Akad. Nauk SSSR, Fiz. Atmos. Okeana* **16** (6), 643–646 (1980).
14. N. N. Pertsev, "Seasonal and height variations of orographically induced mesoscale fluctuations in the middle atmosphere," *Izv., Atmos. Ocean. Phys.* **33** (6), 722–728 (1997).
15. N. N. Pertsev, "Azimuthal anisotropy of windward mountain waves in the upper atmosphere," *Izv. Akad. Nauk SSSR, Fiz. Atmos. Okeana* **25** (6), 585–591 (1989).

16. N. N. Pertsev, "Causes and consequences of temperature rise in the hydroxyl layer over mountains," in *Dynamics of the ionosphere* (Gylym, Alma-Ata, 1991), Vol. 3, pp. 165–170 [in Russian].
17. N. M. Gavrilov, "Structure of the mesoscale variability of the troposphere and stratosphere found from radio refraction measurements via CHAMP satellites," *Izv., Atmos. Ocean. Phys.* **43** (4), 451–460 (2007).
18. F. Lott and M. J. Miller, "A new subgrid-scale orographic drag parametrization: its formulation and testing," *Quart. J. R. Meteorol. Soc.* **123** (537), 101–127 (1997).
19. J. F. Scinocca and N. A. McFarlane, "The parametrization of drag induced by stratified flow over anisotropic orography," *Quart. J. R. Meteorol. Soc.* **126** (568), 2353–2393 (2000).
20. N. M. Gavrilov, "Parametrization of the dynamical and thermal effect of steady-state internal gravity waves on the middle atmosphere," *Izv. Akad. Nauk SSSR, Fiz. Atmos. Okeana* **25** (3), 271–278 (1989).
21. E. E. Gossard and W. H. Hooke, *Waves in the Atmosphere: Atmospheric Infrasound and Gravity Waves: Their Generation and Propagation* (Elsevier, Amsterdam/New York, 1975; Mir, Moscow, 1978).
22. D. S. Phillips, "Analytical surface pressure and drag for linear hydrostatic flow over three-dimensional elliptical mountains," *J. Atm. Sci.* **41**, 1073–1084 (1984).
23. N. M. Gavrilov, A. I. Pogorel'tsev, and C. Jacobi, "Numerical modeling of the effect of latitude-inhomogeneous gravity waves on the circulation of the middle atmosphere," *Izv., Atmos. Ocean. Phys.* **41** (1), 9–18 (2005).
24. A. E. Hedin, "Extension of the MSIS Thermosphere Model into the middle and lower atmosphere," *J. Geophys. Res.* **96** (A2), 1159–1172 (1991). doi 10.1029/90JA02125
25. R. Kistler, E. Kalnay, W. Collins, et al., "The NCEP-NCAR 50-year reanalysis," *Bull. Am. Meteorol. Soc.* **82** (2), 247–268 (2001).

*Translated by N. Tret'yakova*